
A Scalable Lift-and-Project Differentiable Approach For the Maximum Cut Problem

Ismail Alkhouri¹, Mian Wu², Cunxi Yu³, Jia Liu²,
Rongrong Wang^{†4,5}, Alvaro Velasquez^{†6}

¹Department of Electrical Engineering & Computer Science - University of Michigan

²Department of Electrical & Computer Engineering - Ohio State University

³Department of Electrical & Computer Engineering - University of Maryland

⁴Department of Computational Mathematics, Science, & Engineering - Michigan State University

⁵Department of Mathematical Sciences - Michigan State University

⁶Department of Computer Science - University of Colorado Boulder

[†]Equal last authorship

Abstract

We propose a scalable framework for solving the Maximum Cut (MaxCut) problem in large graphs using projected gradient ascent on quadratic objectives. Notably, while our approach is differentiable and leverages GPUs for gradient-based optimization, it is not a machine learning method and does not require training data beyond the given problem formulation. Starting from a continuous relaxation of the classical quadratic binary formulation, we present a parallelized strategy that explores multiple initialization vectors in batch, offering an efficient and memory-friendly alternative to traditional solvers. We analyze the relaxed objective, showing it is convex and has fixed-points corresponding to local optima—particularly at boundary points—highlighting a key challenge in non-convex optimization. To address this, we introduce a lifted quadratic formulation that over-parameterizes the solution space, allowing the algorithm to escape poor fixed-points. We also provide a theoretical characterization of these lifted fixed-points. Finally, we propose DECO, a dimension-alternating algorithm that switches between the unlifted and lifted formulations, leveraging their complementary strengths along with importance-based degree initialization and a population-based evolutionary hyperparameter search. Experiments on diverse graph families show that our methods attain comparable or superior performance relative to recent training-data-intensive, dataless, and GPU-accelerated sampling approaches.

1 Introduction

A fundamental connection between Combinatorial Optimization Problems (COPs) and NP-hardness was established in the influential work of Karp in [20], highlighting their intrinsic computational difficulty. The paper also introduced the concept of reducibility among NP-complete COPs, allowing their relative complexity to be examined through reductions between problems.

Although there could be a straightforward reduction between some COPs – such as reducing the Maximum Cut (MaxCut) and the Not-all-equal 3-satisfiability (NAE 3SAT) [27] – which allows a solution for one problem to be used to solve another, other COPs differ significantly. For example, there does not exist a direct reduction between MaxCut and the Kidney Exchange Problem (KEP) [26].

In this work, we focus on the MaxCut problem, a fundamental COP with wide-ranging applications. These include, but are not limited to, interference management in wireless networks [15], physical design in VLSI circuits [23], and ensuring consistency in phylogenetic tree construction in biology [33].

The Maximum Cut (MaxCut) problem partitions the set of nodes V of graph $G = (V, E)$ into two disjoint sets, such that the number of edges crossing between the two sets is maximized. Several methods have been proposed to tackle the MaxCut problem, including the ones based on Integer Linear Programming (ILP) [25] and Quadratic Unconstrained Binary Optimization (QUBO) [13]. However, as ILP and QUBO formulations rely on integer variables, they do not scale well, often incurring high computational costs on large or dense graphs. Heuristic approaches, such as Breakout Local Search (BLS) [4], offer faster solutions but generally lack theoretical guarantees and of-

ten require problem-specific and graph-specific tuning. A widely known approximation algorithm based on semidefinite programming (SDP) was introduced by Goemans and Williamson [14], providing strong theoretical guarantees. However, the SDP solution must be rounded to obtain a valid cut, and such rounding may result in suboptimal solutions.

Recent years have seen a surge in learning-based approaches for MaxCut and other COPs, including supervised, unsupervised, and reinforcement learning methods [5, 1, 36]. While these methods have shown promise, they typically require a large amount of labeled or unlabeled training graphs. As a result, many of them often generalize poorly to out-of-distribution (OOD) instances and struggle to scale to larger graphs, even from the same distribution (see the results of DIFUSCO [35] on the large graphs in [3]). To address these limitations, training-data-free (or data-less) graph neural network (GNN) methods have been proposed [32, 18], where the GNN parameters are optimized using a relaxed QUBO formulation over the single graph that defines the given problem instance. However, some of these methods remain constrained by input encodings that hinder scalability and typically only perform well on relatively sparse graphs.

An alternative class of data-less approaches—those based on GPU-accelerated optimization or sampling methods—has recently emerged [3, 34, 22]. These methods avoid both the need for training data and the graph encoding bottlenecks of GNN-based techniques, and have demonstrated competitive performance, even against state-of-the-art problem-specific heuristics. However, they often rely on hand-tuned hyper-parameters (typically a small set of scalar values) to achieve strong performance.

In parallel, the increasing capabilities of modern GPUs, as well as advances in distributed and parallel computing, have enabled solvers based on differentiable frameworks—such as the method based on Gumbel-softmax presented in [24]—to outperform traditional CPU-bound solvers, including commercial packages like Gurobi [16] and CP-SAT [30], on large-scale scheduling COPs.

Motivated by the benefits of GPU-based parallel computation and the flexibility of training-data-free optimization, this paper proposes two data-less differentiable quadratic formulations for the MaxCut problem, along with an alternating optimization algorithm. The first formulation is a relaxed QUBO, while the second introduces a lifted quadratic optimization. The contributions of the paper are summarized as follows:

1. **Relaxed and Lifted Formulations:** We propose a relaxed unlifted QUBO formulation and introduce a lifted quadratic formulation that over-parameterizes the solution space.

2. **Theoretical Insights:** We provide theoretical insights into the relaxed unlifted objective, including convexity of the objective, the graph Laplacian and its null space. We identify two types of fixed-points including boundary points that explain why local minima arise in those settings. Furthermore, we theoretically characterize the MaxCut lifted fixed-points.
3. **Scalable Parallelized Algorithms:** Building on these formulations and fixed-point characterizations, we develop three GPU-parallelized scalable algorithms, including a dimension-alternating scheme that switches between the unlifted and lifted formulations.
4. **Initialization and Hyper-Parameter Search:** To mitigate sensitivity to initial vectors and reduce manual tuning, we adopt an importance-based initialization strategy and employ a population-based evolutionary algorithm for parameter search.
5. **Extensive Empirical Evaluation:** On large graph datasets, we show that our objectives—combined with batching, degree-based initialization, and hyper-parameter search—achieve competitive MaxCut solutions at scale. Our results suggest that differentiable, parallelized, and training-data-free approaches can rival or surpass data-intensive and recent sampling-based methods.

2 Preliminaries

Notations: Let $G = (V, E)$ be an undirected graph, where V is the set of nodes and $E \subseteq V \times V$ is the set of edges. The number of nodes and edges are denoted by $|V| = n$ and $|E| = m$, respectively, where $|\cdot|$ indicates the cardinality of a set. For a node $v \in V$, its degree d_v is the number of edges connected to v , and the maximum degree in the graph is denoted by Δ . The symmetric adjacency matrix of the graph is denoted by $\mathbf{A} \in \{0, 1\}^{n \times n}$, where $\mathbf{A}_{u,v} = 1$ if $(u, v) \in E$ and 0 otherwise. The identity matrix is denoted by \mathbf{I} . The diagonal degree matrix is $\mathbf{D} \in \{0, 1\}^{n \times n}$, where $\mathbf{D}_{v,v} = d_v$. The trace of a matrix \mathbf{A} is denoted by $\text{tr}(\mathbf{A})$. For any positive integer n , we use $[n] := \{1, \dots, n\}$. The vector of all ones of size n is denoted by \mathbf{e}_n and the vector of all zeros is denoted by $\mathbf{0}_n$. We also use $\mathbb{1}\{\cdot\}$ to denote the indicator function, which returns 1 if its argument is true and 0 otherwise. We now formally define the NP-hard problem of finding a Maximum Cut (MaxCut) in a graph.

Definition 1 (Maximum Cut (MaxCut)). *Given an undirected graph $G = (V, E)$, the goal of the MaxCut problem is to partition the nodes into two disjoint sets S and $\bar{S} = V \setminus S$ such that the number of edges crossing the cut (i.e., with one endpoint in S and the other in \bar{S}) is maximized.*

Given any set $S \subset V$, the cut value is defined as:

$$\text{Cut}(S) = \sum_{v \in S} \sum_{u \in V \setminus S} \mathbb{1}\{(v, u) \in E\}. \quad (1)$$

Let $\mathbf{z} \in \{0, 1\}^n$ be a binary vector where each entry \mathbf{z}_v corresponds to node $v \in V$, and let $\mathbf{y}_{v,u}$ corresponds to an edge $(v, u) \in E$ stacked in an m -dimensional binary vector. Then, the MaxCut problem can be formulated as the following integer linear program (ILP):

$$\begin{aligned} \max_{\mathbf{z} \in \{0,1\}^n, \mathbf{y} \in \{0,1\}^m} \quad & \sum_{(v,u) \in E} \mathbf{y}_{v,u} \\ \text{s.t.} \quad & \mathbf{y}_{v,u} \leq \mathbf{z}_v + \mathbf{z}_u, \\ & \mathbf{y}_{v,u} \leq 2 - \mathbf{z}_v - \mathbf{z}_u, \quad \forall (v, u) \in E. \end{aligned} \quad (2)$$

Let \mathbf{y}^* be the optimal solution to (2). Then, the optimal cut value is $\sum_{(v,u) \in E} \mathbf{y}_{v,u}^*$. This ILP involves $n + m$ binary variables. An alternative formulation that uses only n binary variables is the following Quadratic Unconstrained Binary Optimization (QUBO), where the optimal cut value is equal to the value of the objective:

$$\max_{\mathbf{z} \in \{-1,1\}^n} \frac{1}{2} \sum_{(v,u) \in E} (\mathbf{z}_v - \mathbf{z}_u)^2. \quad (3)$$

Since both (2) and (3) are binary programs, they scale poorly with increasing n and m . To address this, lifting-based relaxations have been explored—most notably, the following semidefinite programming (SDP) relaxation of MaxCut:

$$\begin{aligned} \max_{\mathbf{W} \in \mathbb{R}^{n \times n}} \quad & \frac{1}{2} \sum_{(v,u) \in E} (1 - \mathbf{W}_{v,:}^\top \mathbf{W}_{u,:}) \\ \text{s.t.} \quad & \mathbf{W}_{v,v} = 1, \quad \forall v \in V, \\ & \mathbf{W} \succeq 0, \end{aligned} \quad (4)$$

where $\mathbf{W}_{v,:}$ denotes the v -th column of \mathbf{W} . While (4) is convex and solvable in polynomial time, it has two primary limitations: (i) a rounding procedure is required to map the solution \mathbf{W}^* to a feasible cut in the original graph, often yielding suboptimal results; and (ii) scalability issues arise as n increases, due to the positive semidefinite constraint $\mathbf{W} \succeq 0$. To address the first limitation, Goemans and Williamson [14] proposed a rounding algorithm—known as the Goemans-Williamson (GW) algorithm—that samples a random hyperplane through the origin and partitions the node embeddings accordingly. This method guarantees, in expectation, a cut value that is at least 0.878 times the optimal value.

3 Proposed Objective Functions

In this section, we introduce a relaxed quadratic objective for MaxCut, describe its optimization using gradient ascent, characterize its behavior, propose a lifted quadratic

formulation to improve exploration, and characterize the lifted fixed-points.

3.1 Differentiable Quadratic Optimization

Let $\mathbf{x} \in [-1, 1]^n$ be a vector where each entry \mathbf{x}_v corresponds to node $v \in V$. A relaxed version of the QUBO formulation in (3) can be written as:

$$\begin{aligned} \max_{\mathbf{x} \in [-1,1]^n} \quad & f(\mathbf{x}) =: \frac{1}{2} \sum_{(v,u) \in E} (\mathbf{x}_v - \mathbf{x}_u)^2 \\ & = \mathbf{x}^\top (\mathbf{D} - \mathbf{A}) \mathbf{x} = \mathbf{x}^\top \mathbf{L} \mathbf{x}, \quad (\text{QUCO}) \end{aligned}$$

where \mathbf{L} is the graph Laplacian. An equivalent form is derived by expanding the objective:

$$\frac{1}{2} \sum_{(v,u) \in E} (\mathbf{x}_v - \mathbf{x}_u)^2 = \sum_{v \in V} d_v \mathbf{x}_v^2 - \sum_{(u,v) \in E} \mathbf{x}_v \mathbf{x}_u.$$

We term this formulation as QUadratic box-Constrained Optimization (QUCO). Notably, if \mathbf{x} lies at the boundary (i.e., entries in $\{-1, 1\}$), then the objective function is equivalent to the objective of the binary program in (3). Let $\mathbf{z} \in \{0, 1\}^n$ represent the binarized version of $\mathbf{x} \in [-1, 1]^n$, i.e.,

$$\mathbf{z}_v = \mathbb{1}\{\mathbf{x}_v > 0\}, \text{ then the cut value is } \mathbf{z}^\top \mathbf{L} \mathbf{z}. \quad (5)$$

The recent study in [3] showed that using projected gradient descent with a relaxed box-constrained version of the Maximum Independent Set (MIS) QUBO with a modified formulation yields better and/or competitive solutions against several state-of-the-art (SOTA) learning-based and sampling-based methods. Motivated by this, in this paper, we first propose to solve (QUCO) using projected gradient ascent.

To this end, let the gradient of f be denoted as

$$\mathbf{g}(\mathbf{x}) =: \nabla_{\mathbf{x}} f(\mathbf{x}) = \mathbf{L} \mathbf{x}.$$

Starting from an initial point \mathbf{x} , the updates in (6) are run for T iterations.

$$\mathbf{x} \leftarrow \text{Proj}_{[-1,1]}(\mathbf{x} + \alpha \mathbf{g}(\mathbf{x})), \quad (6)$$

where $\alpha > 0$ is the step size and the projection operator is applied element-wise. We next state two properties of the graph Laplacian \mathbf{L} .

Lemma 1. *For any graph with one connected component, \mathbf{L} is positive semidefinite (PSD).*

Lemma 2. *For any graph with one connected component, the null space of \mathbf{L} ,*

$$N(\mathbf{L}) = \{\mathbf{x} \in \mathbb{R}^n : \mathbf{L} \mathbf{x} = \mathbf{0}\},$$

is one-dimensional, spanned by the all-ones vector \mathbf{e}_n .

Lemma 1 follows from the non-negativity of the objective of (QUCO) as we have $\sum_{(v,u) \in E} (\mathbf{x}_v - \mathbf{x}_u)^2 \geq 0$. Lemma 2 holds due to the row-sum property of \mathbf{L} (each row or column sums up to 0) [6].

As a direct result of Lemma 1, f is convex as \mathbf{L} is PSD. A direct result of Lemma 2 is that for any $c \in \mathbb{R}$, we have $c\mathbf{e}_n \in N(\mathbf{L})$.

Although the projection operator in (6) does not affect the convexity of f , it creates **fixed-points** that could correspond to different graph cuts. Finding the optimal MaxCut fixed-point(s) is NP-hard in general.

Remark 1. *Since we are solving the MaxCut problem, we assume that the graph G has only one connected component, i.e., there is a path from any two nodes. If the graph has multiple connected components, then MaxCut can be solved independently on each component.*

Due to the absence of a linear term in f , any vector in the null space of \mathbf{L} creates a fixed-point that is a stationary point (i.e., $\mathbf{g}(\mathbf{x}) = \mathbf{0}$). Next, we formally define the MaxCut fixed-points of (QUCO).

Definition 2 (MaxCut fixed-points). *For any graph with one connected component $G = (V, E)$, define the set of MaxCut fixed-points as*

$$F := \left\{ \mathbf{x} \in \{-1, 1\}^n \setminus N(\mathbf{L}) \quad \text{such that} \right. \\ \left. \mathbf{x} = \text{Proj}_{[-1,1]}(\mathbf{x} + \alpha \mathbf{g}(\mathbf{x})) \right\}. \quad (7)$$

That is, F contains binary vectors that are not in the null space of \mathbf{L} but remain unchanged after a gradient ascent step followed by projection. Any point in the interior of the box (i.e., $(-1, 1)^n$) cannot be a MaxCut fixed-point unless it lies in the null space.

The above definition indicates that any point in F corresponds to a “local maximizer” of (QUCO) in the sense that a projected gradient ascent step returns the exact same point.

3.2 Lifted Quadratic Formulation

Inspired by over-parameterization in machine learning, which is known to improve optimization landscapes and escape suboptimal maxima [7, 29] and since gradient ascent on the unlifted objective (QUCO) often gets stuck at fixed-points and fails to explore other potentially better cuts, we propose a lifted quadratic optimization formulation.

More specifically, we represent each node $v \in V$ using an l -dimensional vector. Here, $l \leq n$ is the lifting parameter. Our proposed Lifted qUadratic Optimization (LUCO) is:

$$\max_{\mathbf{X} \in [-1,1]^{n \times l}} h(\mathbf{X}) =: \text{tr}(\mathbf{X}^\top \mathbf{L} \mathbf{X}). \quad (\text{LUCO})$$

The Jacobian is

$$\mathbf{J}(\mathbf{X}) \in \mathbb{R}^{n \times l} = \mathbf{L} \mathbf{X},$$

and the update rule of the gradient ascent becomes:

$$\mathbf{X} \leftarrow \text{Proj}_{[-1,1]}(\mathbf{X} + \alpha \mathbf{J}(\mathbf{X})). \quad (8)$$

Assuming the above updates converge to a fixed-point, the resulting cut value is computed via:

$$\mathbf{z}_v = \mathbb{1} \left\{ \sum_{i \in [l]} \mathbf{X}_{v,i} \geq 0 \right\}, \quad \text{with cut value of } \mathbf{z}^\top \mathbf{L} \mathbf{z}. \quad (9)$$

In (9), we check whether the sum of row v in \mathbf{X} is greater than or equal to 0. In the following theorem, we characterize the lifted MaxCut fixed-points based on which points do not yield an all-zero Jacobian. The proof is deferred to the Appendix A.

Theorem 1 (Lifted MaxCut fixed-points). *Given a graph $G = (V, E)$ with one connected component, its Laplacian matrix \mathbf{L} , and the gradient ascent updates in (8), then, according to (9), the set of fixed-points that correspond to MaxCut is*

$$P := \left\{ \mathbf{X} \in \{-1, 1\}^{n \times l} : \mathbf{X} \neq \mathbf{e}_n \mathbf{c}^\top, \mathbf{c} \in \mathbb{R}^l \right\}. \quad (10)$$

This result excludes vectors where all rows of \mathbf{X} are identical (i.e., lie in the null space of \mathbf{L}), which would yield a cut value of zero.

Remark 2. *Compared to solving the MaxCut SDP in (4), (LUCO) avoids the need to enforce the PSD constraints and the $|V|$ equality constraints. Moreover, the lifting dimension, l , does not need to be explicitly enforced to be equal to n , as is the case with SDP. In both the MaxCut SDP and our proposed objective in (LUCO), a rounding is needed. Empirically, we will show that QUCO and LUCO are better suited for large-scale graphs where enforcing PSD constraints becomes computationally prohibitive—even when using commercial SDP solvers such as MOSEK [28].*

Remark 3. *A recent learning-based method also introduces a lifted version for the MaxCut problem, where the PSD constraints in (4) are replaced by the ℓ_2 norm on each column of the optimization matrix [36]. Then, the authors define a connection between message passing of GNNs [11] and applying gradient descent on their lifted formulation. There are two differences between our lifted formulation and the one in [36]: (i) Our formulation uses only box-constraints, whereas an ℓ_2 norm is needed in [36]; and more importantly (ii) the method in [36] embeds trainable weight matrices in every layer that represents the aggregate function of the GNN, and trains over training graphs, whereas our method is not a learning-based approach that avoids any potential generalizability issues typically encountered in training-data-intensive methods [37].*

4 Proposed Algorithms

In this section, we first introduce two degree-based initialization strategies, followed by the three proposed parallelized algorithms based on the formulations in (QUCO) and

(LUCO). Then, we describe the adopted evolution-based hyper-parameter search algorithm.

4.1 Degree-based Initialization

We consider two degree-based initialization strategies, where the motivation is that high-degree nodes have greater influence on the cut value when switching between partitions.

Degree-based via Uniform Distribution Initialization (DUI): Here, higher-degree nodes are initialized with values closer to zero than lower-degree nodes. Specifically, we define:

$$\mathbf{h}_{\text{DUI}} \sim \mathcal{U} \left[- \left(1 - \frac{d_v}{\bar{d}} \right), \left(1 - \frac{d_v}{\bar{d}} \right) \right]^n,$$

where \mathcal{U} denotes the continuous uniform distribution.

Importance-based Degree-based Initialization (IDI): Here, the nodes are first divided into important and less important (or unimportant) sets based on the graph average degree and d_v . Then, two types of node assignments are used to sample from the discrete uniform distribution $\mathcal{U}\{-1, 1\}$ to construct \mathbf{h}_{IDI} . This approach is inspired by the above direct degree-based distribution sampling and the local search metaheuristic algorithm in [10, 9, 8]. More specifically, we first divide V into an important set

$$I := \{v \in V : d_v > \bar{d} + \beta\sigma\},$$

and an unimportant set $U = V \setminus I$, where

$$\bar{d} = \frac{1}{|V|} \sum_{v \in V} d_v, \quad \sigma^2 = \frac{1}{|V|} \sum_{v \in V} (d_v - \bar{d})^2$$

is the mean degree of the graph and σ^2 is the variance. Here, $\beta \in (0, 1)$ is a threshold. We initialize the nodes in the important set using the discrete uniform distribution, i.e., for each $i \in I$, $p_i \sim \mathcal{U}\{-1, 1\}$. Consequently, we use p_i to initialize the nodes in the unimportant set as follows. First, define indicator vectors $\mathbf{a}, \mathbf{b} \in \{0, 1\}^n$ such that $\mathbf{a}_i = \mathbb{1}\{p_i = 1\}$, $\mathbf{b}_i = \mathbb{1}\{p_i = -1\}$. We have $(\mathbf{A}\mathbf{a})_i$ (resp. $(\mathbf{A}\mathbf{b})_i$) indicates the number of the edges from node i to the important (resp. unimportant) nodes. Then, for every node in the unimportant set, i.e., $i \in U$, we have

$$r_i = \begin{cases} \sim \mathcal{U}\{-1, 1\}, & \text{if } (\mathbf{A}\mathbf{a})_i = (\mathbf{A}\mathbf{b})_i, \\ +1, & \text{if } (\mathbf{A}\mathbf{a})_i < (\mathbf{A}\mathbf{b})_i, \\ -1, & \text{otherwise,} \end{cases}$$

That is, if the cut gain is tied, choose randomly; otherwise assign i to the side with fewer connections to the important nodes. Based on sets I and U , \mathbf{h}_{IDI} is constructed using p_i and r_i .

For the lifted formulation, these initialization strategies are applied to each of the l column vectors in the matrix \mathbf{X} .

4.2 Parallelized Algorithms

To improve scalability, we adopt GPU-accelerated batch execution, where B initialization vectors are processed in parallel. This means that multiple vectors from the above initializations are processed at the same time. For the first batch, we generate Gaussian-distributed vectors centered at \mathbf{h}_{DUI} or \mathbf{h}_{IDI} with covariance matrix $\eta\mathbf{I}$, where $\eta \in \mathbb{R}^+$ is an exploration parameter. For subsequent batches, the mean vector changes to the best binary vector that corresponds to the highest cut value from the previous batch.

The algorithm for optimizing the unlifted formulation (QUCO) using parallel projected gradient ascent is shown in Algorithm 1, referred to as parallelized QUCO or **pQUCO**. We denote the output of this procedure as $\text{pQUCO}(\mathbf{x})$, which returns the best binary vector corresponding to the maximum cut.

Algorithm 2 presents the procedure of parallelized LUCO (pLUCO). Similar to pQUCO, we denote running Algorithm 2 by $\text{pLUCO}(\mathbf{X})$. The output of this function is the binary vector with the largest cut from the lifted run.

We note that while the procedures of both Algorithm 1 and Algorithm 2 describe the use of projected fixed-step-size gradient ascent (PGA), we use momentum-based PGA in practice based on our empirical results.

Dimension-Alternating Quadratic Optimization Algorithm:

Here, we combine the scalability of the unlifted formulation with the exploratory power of the lifted formulation, we propose an alternating approach: the Dimension Alternating Quadratic Optimization algorithm, or DECO. The intuition is as follows: start with a solution from pQUCO, then lift it to a higher-dimensional representation to refine the cut using pLUCO, and then project back to the unlifted representation. This lift-and-project process can be repeated as long as the run-time budget allows. Algorithm 3 presents the procedure.

4.3 Evolution-based Hyper-parameters Search

Motivated by the need to mitigate manual tuning of parameters, namely the step size α and the number of optimization steps T , we adopt an evolution-based parameter search algorithm. The procedure is inspired by the population-based training in Algorithm 1 of [19], where combinations of the hyper-parameters are tried, ranked, and then replaced based on function evaluations and a series of evolution rounds. However, we make modifications because in our algorithms, we only search for two parameters (α and T). We note that this procedure is applied between batches.

Based on pre-defined bounds of α and T , we randomly select pairs from these to construct a population list that we will try next. More specifically, we draw T from the discrete uniform distribution, i.e., $\mathcal{U}\{T_l, T_u\}$. For α , we use 10

Algorithm 1 parallelized QUCO (pQUCO)

Input: Graph $G = (V, E)$, number of initializations B in one batch, number of iterations T , step size α , and initialization method. Initialize \mathbf{x} and $S_{\text{cut}} = \{\cdot\}$ (Empty set to collect MaxCut sets).

- 1: **For** each of the B vectors, **Do** (Parallel Execution)
 - 2: **For** T iterations, **Do** (Gradient updates)
 - 3: $\mathbf{x} \leftarrow \text{Proj}_{[-1,1]}(\mathbf{x} + \alpha \mathbf{g}(\mathbf{x}))$
 - 4: $\mathbf{z}_v = \mathbb{1}\{\mathbf{x}_v > 0\}$ (Binarization)
 - 5: $S_{\text{cut}} \leftarrow S_{\text{cut}} \cup \{v \in V : \mathbf{z}_v = 1\}$
 - 6: **return:** $S^* = \arg \max_{S \in S_{\text{cut}}} \text{Cut}(S)$
-

to an exponent e that is uniformly sampled from $\mathcal{U}[e_l, e_u]$.

Based on the number of generations (or evolutions), we first solve for all combinations inside the population; Keep the top half and replace the bottom half. The number of evolutions indicate the number of rounds used to update the list of combinations inside the population list. Next, we explain the way of replacing the bottom half of combinations that is applied for each round.

For each combination we want to replace, we perturb a pair from the set of combinations the we want to keep and then clip it to the bounded values. More specifically, for α , let e be the exponent from a pair that we will keep in the next round. Let e' be the exponent we will include in the next round which is obtained based on a perturbed e as

$$e' = \text{Proj}_{[-4,-1]}[e + 0.2\epsilon], \text{ where } \epsilon \sim \mathcal{N}(0, 1).$$

For the step size, let T_0 be a step size selected from the combinations we will keep in the next round of evolutions which will be used to obtain T' . Here, T' is the one used to replace a step size from the bottom half of the population set. T' is obtained from T_0 as

$$T' = \lfloor T_0(1 + 0.2(2\epsilon' - 1)) \rfloor,$$

where $\epsilon' \sim \mathcal{U}(0, 1)$, and $\lfloor \cdot \rfloor$ is the integer function.

At the end of the algorithm, the best α and T are selected for the next batch. The impact of adopting this algorithm is given in the Ablation study of Appendix B.

5 Experimental Results

5.1 Settings

We code our algorithms using PyTorch. For baselines, we consider: (i) exact solvers Gurobi [16] and CP-SAT [30] for the ILP in (2); (ii) training-data-intensive methods, LwD [2] (reinforcement learning) and OptGNN [36] (unsupervised learning); (iii) GNN-based training-data-free methods, PIGNN [32] and CRA [18]; and (iv) recent GPU-based sampling method ReSCO [22]. Furthermore, we consider

Algorithm 2 parallelized LUCO (pLUCO)

Input: Graph $G = (V, E)$, number of initializations B in one batch, number of iterations T , step size α , lifting parameter l , and initialization method. Initialize \mathbf{X} and $S_{\text{cut}} = \{\cdot\}$ (Empty set to collect MaxCut sets).

- 1: **For** each of the B vectors, **Do** (Parallel Execution)
 - 2: **For** T iterations, **Do** (Gradient updates)
 - 3: $\mathbf{X} \leftarrow \text{Proj}_{[-1,1]}(\mathbf{X} + \alpha \mathbf{J}(\mathbf{X}))$
 - 4: $\mathbf{z}_v = \mathbb{1}\{\sum_{i \in [l]} \mathbf{X}_{v,i} \geq 0\}$ (Binarization)
 - 5: $S_{\text{cut}} \leftarrow S_{\text{cut}} \cup \{v \in V : \mathbf{z}_v = 1\}$
 - 6: **return:** $S^* = \arg \max_{S \in S_{\text{cut}}} \text{Cut}(S)$
-

Algorithm 3 parallelized DECO (pDECO)

Input: Graph $G = (V, E)$, number of initializations B in one batch, number of iterations T , step size α , lifting parameter l , and initialization method (DUI or IDI). Initialize \mathbf{x} and $S_{\text{cut}} = \{\cdot\}$ (Empty set to collect MaxCut sets).

- 1: **Obtain** $\mathbf{x} \leftarrow \text{pCQO}(\mathbf{x})$ (running pQUCO)
 - 2: **Initialize** each column of \mathbf{X} based on initialization method.
 - 3: $\mathbf{x} \leftarrow \text{pLUCO}(\mathbf{X})$ (running pLUCO)
 - 4: **Repeat** from Step 1 until the time budget expires.
-

a parallelized version of the GW algorithm [14] (which we term by SDP+pGW) that uses the MOSEK solver in [28] to first obtain the solution of (4), then solves several initializations in parallel using batching and GPUs. For all of these methods, we use the default code bases. For LwD and OptGNN, we provide more details about their implementations of the in Appendix C. All of the experiments were conducted on an H100 GPU machine.

For the initialization of our algorithms (DUI and IDI), we scale the initial vectors down by a large factor (e.g., 10,000), as we empirically observed that this leads to more stable optimization with respect to both the number of steps T and the step size α . This observation is consistent with findings in neural network initialization literature, where improper scaling can cause exploding or vanishing gradients, negatively impacting convergence. For example, the well-known AlexNet [21] relied on scaling and normalization techniques to stabilize early training. More formal analyses are given in the Xavier initialization [12] and He initialization [17]. These results support our observation that scaling down the initialization improves the stability of gradient-based updates in our setting.

For graph datasets, we consider (i) Erdos-Renyi (ER) small dataset consisting of 128 graphs with 700 to 800 nodes and probability of edge creation $p = 0.15$ (which indicates that nearly 15% of possible edges from the complete graph exist) [3]; (ii) 19 graphs from the well-known dataset, Gset¹, with number of nodes ranging from 800 to 2000 and number of edges ranging from 500 to 40,000; (iii) Very large ER graph dataset that consists of 15 graphs with 20,000 to

¹<http://web.stanford.edu/~yyye/fyye/Gset/>

Solver	Avg. Cut Value	Avg. Run-time (s)
SDP+pGW	23980.67	16.67
Gurobi	22014.84	30.01
CP-SAT	22288.09	9.16
LwD	22356.57	65.24
OptGNN	20385.34	109.26
ReSCO	22569.92	81.65
PIGNN	22454.29	67.74
CRA	22688.29	78.43
pQUCO+DUI	20276.83	46.88
pQUCO+IDI	22992.16	57.35
pLUCO+DUI	18552.57	83.29
pLUCO+IDI	22237.51	98.21
pDECO+DUI	20853.76	216.14
pDECO+IDI	22865.41	254.92

Table 1: Average results of the **small ER dataset** with $p = 0.15$ from [31]. ‘DUI’ and ‘IDI’ correspond to the two initializations strategies.

Solver	Avg. Cut Value	Avg. Run-time (s)
SDP+pGW	–	–
Gurobi	9628.31	82.99
CP-SAT	9630.53	53.15
LwD	7876.54	167.74
OptGNN	6851.25	211.17
ReSCO	8381.53	131.25
PIGNN	7739.51	94.56
CRA	8481.23	196.54
pQUCO+DUI	6987.95	175.34
pQUCO+IDI	8457.25	199.23
pLUCO+DUI	6835.37	185.39
pLUCO+IDI	7678.41	232.56
pDECO+DUI	7123.27	273.10
pDECO+IDI	8846.35	352.23

Table 2: Results on the **Gset** dataset. For acronyms, see the caption of Table 1. “–” indicates that MOSEK was not able to solve the SDP due to running out of memory.

30,000 nodes and $p = 0.1$ (with number of edges ranging from 19,999,000 to 44,998,500). These graphs were generated by the ER NetworkX random graph generator².

For pLUCO and pDECO, we use $l = 2$ as our lifting dimension following the ablation study in Table 4 in the Appendix. For the IDI initialization, we use $\beta = 0.2$. For the exploration parameter, we use $\eta = 0.8$. For the momentum in PGA, we use 0.9.

For the adopted evolution-based hyper-parameter search, we use $T_l = 3000$, $T_u = 10000$, $e_l = -4$, and $e_u = -1$. The population size is 6 and the number of evolution rounds is set to 5. Our code is available online³.

²<https://networkx.org/documentation/stable/reference/generators.html>

³https://anonymous.4open.science/r/GD_maxcut-65D6/README.md

Solver	Avg. Cut Value	Avg. Run-time (s)
SDP+pGW	–	–
Gurobi	–	–
CP-SAT	–	–
LwD	–	–
OptGNN	–	–
ReSCO	25220597.48	22523.46
PIGNN	25223415.89	1214.55
CRA	25230787.14	1677.38
pQUCO+DUI	23032986.33	4896.10
pQUCO+IDI	25312959.41	5577.24
pLUCO+DUI	21896472.81	5631.73
pLUCO+IDI	23360609.38	6475.40
pDECO+DUI	23252076.92	9483.70
pDECO+IDI	25407655.15	10972.48

Table 3: Results on **Large Scale ER** with $p = 0.1$. “–” indicates that this method does not return any results, requires significant amount of time, or due to running out of memory.

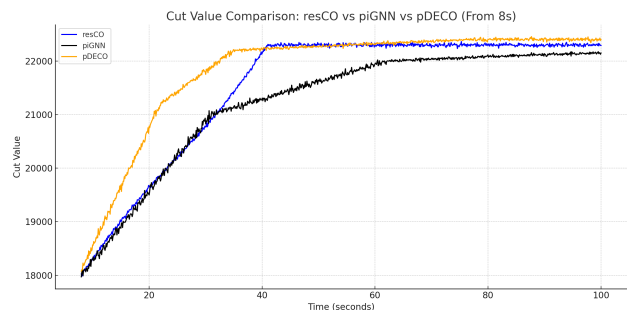


Figure 1: Convergence of our method (pDECO), ReSCO, and PIGNN over 100 seconds (x-axis). The y-axis corresponds to the cut value of the average of five graphs from the small ER dataset.

5.2 Main Results

5.2.1 Comparison Results

Table 1, Table 2, and Table 3 present the results for the small ER, Gset, and large ER graph datasets, respectively. We note that the entries with “–” in the tables indicate that this method does not return any results due to running out of memory or requiring a significantly large amount of time given the used compute.

In general, all DUI initializations achieve less average cut value than the IDI initialization while requiring less runtime, which is observed on all datasets. This shows the impact of the adopted importance-based initialization.

In Table 1, among our methods, pQUCO with IDI initialization achieved an average cut of 22992.16, surpassing all LUCO and DECO variants without search by at least 400. Although SDP+pGW achieved the highest cut value (23980.67) with a runtime of 16.7 s, it does not scale to larger graphs as seen in Table 2 and Table 3. The reason is that enforcing the PSD constraint in (4) becomes harder on larger graphs. Our pDECO+IDI reached 22865.41, only 4.6% below SDP+pGW. Most of our algorithms outper-

Method	Dataset	(n, p)	$l = 2$		$l = 3$		$l = n$	
			Cut Value	Run-time (s)	Cut Value	Run-time (s)	Cut Value	Run-time (s)
pLUCO	Small ER	(700, 0.15)	20894.35	50.39	20951.80	57.13	22201.47	68.60
	Small ER	(800, 0.15)	21734.11	66.33	21805.49	71.33	22457.81	81.45
	large ER	(20000, 0.1)	2330278.41	5042.5	23347681.55	5611.89	-	-
	large ER	(30000, 0.1)	24606401.05	7077.36	24630531.38	7735.23	-	-
pDECO	Small ER	(700, 0.15)	22431.85	335.44	22793.48	354.21	22385.71	405.41
	Small ER	(800, 0.15)	22589.35	347.87	23034.17	371.64	22476.23	442.50
	large ER	(20000, 0.1)	25344652.38	9560.23	25394246.13	10581.74	-	-
	large ER	(30000, 0.1)	25731427.59	9986.37	25814245.25	11074.65	-	-

Table 4: Ablation study on using different values of the lifting parameter l in pLUCO and pDECO.

form OptGNN in both cut value and run-time without requiring any training data or a neural network. pDECO+IDI and pQUCO+IDI outperform LwD, also without the need of any training data or an RL agent.

On the Gset dataset (Table 2), our pDECO+IDI produced the best cut among all our approaches (8846.35) and improved over pQUCO (which reports 8457.25 at best). This demonstrates the benefit of our dimension-alternating approach in Algorithm 3. pDECO+IDI also outperformed all of the neural-network-based methods (LwD, OptGNN, PIGNN, and CRA). For Gset, exact solvers (Gurobi and CP-SAT) achieved highest cuts and the lowest run-times. Notably, the ReSCO method based on differentiable sampling achieved 8382 but at a runtime of 131.25 s, whereas pDECO+IDI achieved a much higher cut (8846) at a longer runtime of 352 s, indicating that our alternating strategy remains competitive with state-of-the-art GPU-accelerated sampling methods.

For the largest graphs (Table 3), exact solvers and learning-based methods failed to run (denoted by “-”). Among GPU-based methods, our pDECO+IDI achieved the highest average cut value, surpassing ReSCO while being more than 2x faster. The lifted variants pLUCO+IDI and the unlifted pQUCO+IDI also reached competitive values with significantly less run-time than PIGNN and ReSCO. The dimension-alternating algorithm pDECO consistently offered the best trade-off between cut quality and scalability.

5.2.2 Convergence Results

In Figure 1, we show the convergence of pDECO, ReSCO, and PIGNN over 100 seconds. The results correspond to the average cut value of five graphs from the small ER dataset. We selected ReSCO and PIGNN as baselines due to their scalability, similar to our proposed algorithms.

As observed, our method obtains higher values earlier and also converges to the highest cut values at the 10-second mark.

5.3 Impact of the Lifting Parameter on pLUCO & pDECO

Table 4 investigates the effect of the lifting parameter l . For small ER graphs, increasing l from 2 to n improved pLUCO cuts but increased the run-time as increasing l means more parameters to optimize. For pDECO, $l = 3$ yielded the highest cuts on small ER without excessive run-time, with slight increase for run-time. $l = n$ slightly decreased cut quality.

On large graphs, results show that very high lifting dimensions were computationally prohibitive, confirming that moderate lifting values achieve the best balance. Therefore, for our main results, we used $l = 2$.

6 Conclusion

We introduced a differentiable lift-and-project framework for the MaxCut problem, built on two continuous relaxations: the unlifted quadratic objective (QUCO) and its lifted version (LUCO). Fixed-points for both formulations were theoretically characterized, with QUCO shown to be convex and to admit MaxCut fixed-points at boundary values, and LUCO characterized by a different set of MaxCut fixed-points. We adopted an importance-based initialization and evolution-based parameter search, combined with a parallel gradient-based optimization strategy and dimension alternation. We evaluated our algorithm on small ER graphs, Gset graphs, and very large ER graphs, where we demonstrated that the proposed methods yield competitive cuts while maintaining practical run-times. For the largest graphs, where exact solvers and learning-based baselines did not run, our parallelized dimension-alternating method achieved the best cut values, outperforming other methods and matching the scalability of very recent SOTA GPU-based sampling methods. Overall, these findings suggest that alternating between unlifted and lifted differentiable formulations, combined with batch parallelization, can enhance exploration without requiring training data, offering a scalable alternative for MaxCut on large graphs.

References

- [1] Sungsoo Ahn, Younggyo Seo, and Jinwoo Shin. Learning what to defer for maximum independent sets. In Hal Daumé III and Aarti Singh, editors, *Proceedings of the 37th International Conference on Machine Learning*, volume 119 of *Proceedings of Machine Learning Research*, pages 134–144. PMLR, 13–18 Jul 2020.
- [2] Sungsoo Ahn, Younggyo Seo, and Jinwoo Shin. Learning what to defer for maximum independent sets. In *International Conference on Machine Learning*, pages 134–144. PMLR, 2020.
- [3] Ismail Alkhouri, Cedric Le Denmat, Yingjie Li, Cunxi Yu, Jia Liu, Rongrong Wang, and Alvaro Velasquez. Differentiable quadratic optimization for the maximum independent set problem. In *Forty-second International Conference on Machine Learning*, 2025.
- [4] Una Benlic and Jin-Kao Hao. Breakout local search for the max-cut problem. *Engineering Applications of Artificial Intelligence*, 26(3):1162–1173, 2013.
- [5] Maximilian Böther, Otto Kißig, Martin Taraz, Sarel Cohen, Karen Seidel, and Tobias Friedrich. What’s wrong with deep learning in tree search for combinatorial optimization. *arXiv preprint arXiv:2201.10494*, 2022.
- [6] Fan R. K. Chung. *Spectral Graph Theory*, volume 92 of *CBMS Regional Conference Series in Mathematics*. American Mathematical Society, Providence, RI, 1997.
- [7] Simon Du and Jason Lee. On the power of overparametrization in neural networks with quadratic activation. In *International conference on machine learning*, pages 1329–1338. PMLR, 2018.
- [8] Thomas A Feo and Mauricio GC Resende. A probabilistic heuristic for a computationally difficult set covering problem. *Operations research letters*, 8(2):67–71, 1989.
- [9] Thomas A Feo and Mauricio GC Resende. Greedy randomized adaptive search procedures. *Journal of global optimization*, 6(2):109–133, 1995.
- [10] Paola Festa, Panos M Pardalos, Mauricio GC Resende, and Celso C Ribeiro. Randomized heuristics for the max-cut problem. *Optimization methods and software*, 17(6):1033–1058, 2002.
- [11] Justin Gilmer, Samuel S Schoenholz, Patrick F Riley, Oriol Vinyals, and George E Dahl. Neural message passing for quantum chemistry. In *Proceedings of the 34th International Conference on Machine Learning (ICML)*, 2017.
- [12] Xavier Glorot and Yoshua Bengio. Understanding the difficulty of training deep feedforward neural networks. In *Proceedings of the 13th International Conference on Artificial Intelligence and Statistics*, pages 249–256. JMLR Workshop and Conference Proceedings, 2010.
- [13] Fred Glover, Gary Kochenberger, and Yu Du. A tutorial on formulating and using qubo models. Technical report, University of Colorado, 2019. Includes detailed derivation of the Max-Cut QUBO in Section 3.2.
- [14] Michel X Goemans and David P Williamson. Improved approximation algorithms for maximum cut and satisfiability problems using semidefinite programming. *Journal of the ACM (JACM)*, 42(6):1115–1145, 1995.
- [15] Zhouyou Gu, Branka Vucetic, Kishore Chikkam, Pasquale Aliberti, and Wibowo Hardjawana. Graph representation learning for contention and interference management in wireless networks. *IEEE/ACM Transactions on Networking*, 32(3):2479–2494, 2024.
- [16] Gurobi Optimization, LLC. Gurobi optimizer, 2025.
- [17] Kaiming He, Xiangyu Zhang, Shaoqing Ren, and Jian Sun. Delving deep into rectifiers: Surpassing human-level performance on imagenet classification. In *Proceedings of the IEEE International Conference on Computer Vision*, pages 1026–1034, 2015.
- [18] Yuma Ichikawa. Controlling continuous relaxation for combinatorial optimization. *Advances in Neural Information Processing Systems*, 37:47189–47216, 2024.
- [19] Maxwell Elliot Jaderberg, Wojciech Czarnecki, Timothy Frederick Goldie Green, and Valentin Clement Dalibard. Population based training of neural networks, March 14 2023. US Patent 11,604,985.
- [20] Richard M Karp. Reducibility among combinatorial problems. In *Complexity of computer computations*, pages 85–103. Springer, 1972.
- [21] Alex Krizhevsky, Ilya Sutskever, and Geoffrey E Hinton. Imagenet classification with deep convolutional neural networks. In *Advances in Neural Information Processing Systems*, volume 25, 2012.
- [22] Muheng Li and Ruqi Zhang. Reheated gradient-based discrete sampling for combinatorial optimization. *Transactions on Machine Learning Research*, 2025.
- [23] Frauke Liers, Tim Nieberg, and Gregor Pardella. Via minimization in vlsi chip design-application of a planar max-cut algorithm. 2011.
- [24] Mingju Liu, Yingjie Li, Jiaqi Yin, Zhiru Zhang, and Cunxi Yu. Differentiable combinatorial scheduling at

- scale. In Ruslan Salakhutdinov, Zico Kolter, Katherine Heller, Adrian Weller, Nuria Oliver, Jonathan Scarlett, and Felix Berkenkamp, editors, *Proceedings of the 41st International Conference on Machine Learning*, volume 235 of *Proceedings of Machine Learning Research*, pages 31464–31476. PMLR, 21–27 Jul 2024.
- [25] Cheng Lu and Zhibin Deng. A branch-and-bound algorithm for solving max-k-cut problem. *Journal of Global Optimization*, pages 1–23, 2021.
- [26] Duncan C McElfresh, Hoda Bidkhori, and John P Dickerson. Scalable robust kidney exchange. In *Proceedings of the AAAI Conference on Artificial Intelligence*, volume 33, pages 1077–1084, 2019.
- [27] Bernard ME Moret. Planar nae3sat is in p. *ACM SIGACT News*, 19(2):51–54, 1988.
- [28] MOSEK ApS. *The MOSEK Python Fusion API manual. Version 11.0.*, 2025.
- [29] Behnam Neyshabur, Russ R Salakhutdinov, and Nati Srebro. Path-sgd: Path-normalized optimization in deep neural networks. *Advances in neural information processing systems*, 28, 2015.
- [30] Laurent Perron and Frédéric Didier. Cp-sat.
- [31] Ruizhong Qiu, Zhiqing Sun, and Yiming Yang. Dimes: A differentiable meta solver for combinatorial optimization problems. *Advances in Neural Information Processing Systems*, 35:25531–25546, 2022.
- [32] Martin JA Schuetz, J Kyle Brubaker, and Helmut G Katzgraber. Combinatorial optimization with physics-inspired graph neural networks. *Nature Machine Intelligence*, 4(4):367–377, 2022.
- [33] Sagi Snir and Satish Rao. Using max cut to enhance rooted trees consistency. *IEEE/ACM Transactions on Computational Biology and Bioinformatics*, 3(4):323–333, 2006.
- [34] Haoran Sun, Katayoon Goshvadi, Azade Nova, Dale Schuurmans, and Hanjun Dai. Revisiting sampling for combinatorial optimization. In *International Conference on Machine Learning*, pages 32859–32874. PMLR, 2023.
- [35] Zhiqing Sun and Yiming Yang. Difusco: Graph-based diffusion solvers for combinatorial optimization. *Advances in neural information processing systems*, 36:3706–3731, 2023.
- [36] Morris Yau, Nikolaos Karalias, Eric Lu, Jessica Xu, and Stefanie Jegelka. Are graph neural networks optimal approximation algorithms? In A. Globerson, L. Mackey, D. Belgrave, A. Fan, U. Paquet, J. Tomczak, and C. Zhang, editors, *Advances in Neural Information Processing Systems*, pages 73124–73181. Curran Associates, Inc., 2024.
- [37] Chiyuan Zhang, Samy Bengio, Moritz Hardt, Benjamin Recht, and Oriol Vinyals. Understanding deep learning requires rethinking generalization. In *International Conference on Learning Representations*, 2017.

Appendix

A Proof of Theorem 1

Re-statement of Theorem 1: Given a graph $G = (V, E)$ with one connected component, its Laplacian matrix \mathbf{L} , and the gradient ascent updates in (8), then, according to (9), the set of fixed-points that correspond to MaxCut is

$$P := \left\{ \mathbf{X} \in \{-1, 1\}^{n \times l} : \mathbf{X} \neq \mathbf{e}_n \mathbf{c}^\top, \mathbf{c} \in \mathbb{R}^l \right\}. \quad (11)$$

Proof. We begin the proof by showing that every point $\mathbf{X} = \mathbf{e}_n \mathbf{c}^\top$ (where $\mathbf{c} \in \mathbb{R}^l$) returns a cut value of exactly 0 and therefore is a fixed-point but that is not a MaxCut fixed-point. Then, we show that any $\mathbf{X} \in P$ always returns a cut of strictly more than 0 and its binarized version from (9) is always a fixed-point.

We prove the first part as column-by-column. Let $\mathbf{x} \in [-1, 1]^n$ be an arbitrary column of \mathbf{X} , and assume $\mathbf{L}\mathbf{x} = \mathbf{0}$. Given the objective function of (QUCO), it is clear that the entire sum is zero if and only if each term is zero. That is,

$$\mathbf{x}_v = \mathbf{x}_u \quad \forall (v, u) \in E.$$

Because the graph is connected, every node is reachable from every other node via a sequence of edges. Therefore, this condition implies:

$$\mathbf{x}_1 = \mathbf{x}_2 = \dots = \mathbf{x}_n = c \quad \text{for some } c \in \mathbb{R},$$

i.e., $\mathbf{x} = c\mathbf{e}_n$. Applying this to each column $\mathbf{x}_i, \forall i \in [l]$ of \mathbf{X} , we conclude:

$$\mathbf{X} = \mathbf{e}_n \mathbf{c}^\top \quad \text{for some } \mathbf{c} \in \mathbb{R}^l.$$

Conversely, if $\mathbf{X} = \mathbf{e}_n \mathbf{c}^\top$, then each column of \mathbf{X} lies in the null space of \mathbf{L} , and thus:

$$\mathbf{L}\mathbf{X} = \mathbf{0}_{n \times l}.$$

Applying the RHS of (9) on some $\mathbf{X} = \mathbf{e}_n \mathbf{c}^\top$ results in

$$\mathbf{z}_v = \sum_{i \in [l]} \mathbf{c}_i,$$

which is independent of v and returns either the vector of all-zero or all-one and hence a cut value of exactly 0. This characterization of \mathbf{z} is also used for the second part of the proof, where we have a cut value from (5) that is only 0 when $\mathbf{z} = \mathbf{e}_n$ or $\mathbf{z} = \mathbf{0}_n$. \square

B Impact of the Adopted Parameters Search Algorithm

In this section, we present a study to show the impact of the proposed adoption of the parameters search algorithm discussed in Section 4.3. In this study, we compare our pQUCO, pLUCO, and pDECO versus running versions of the algorithms where the parameters (step size α and number of iterations T) are manually tuned. We list our selection in Table 5. Since we run both the unlifted and lifted formulations in pDECO, we include two tuples in the third column.

Dataset	pQUCO (Algorithm 1)	pLUCO (Algorithm 2)	pDECO (Algorithm 3)
Small ER	(0.15, 48000)	(0.001, 2500)	(0.10, 30000), (0.001, 2000)
Gset	(0.01, 60000)	(0.001, 3000)	(0.012, 80000), (0.001, 2000)
Large Scale ER	(0.01, 100000)	(0.001, 5000)	(0.02, 60000), (0.005, 1000)

Table 5: The values of (α, T) for the ‘‘Manual’’ results in Table 6.

The results are given in Table 6. As observed, using the adopted evolutionary algorithm for tuning the parameters yield better cut values when compared to fixing the parameters to manually tuned settings. However, we note that, in all datasets, using the search algorithm incurs more run-time.

A Scalable Lift-and-Project Differentiable Approach For the Maximum Cut Problem

Method	Hyper-parameter selection	Small ER		Gset		Large ER	
		Avg. Cut Value	Avg. Run-time (s)	Avg. Cut Value	Avg. Run-time (s)	Avg. Cut Value	Avg. Run-time (s)
pQUCO	Manual	22511.44	29.26	7965.63	51.20	25019244.21	991.52
	Automatic	22992.16	57.35	8457.25	19.23	25312959.41	5577.24
pLUCO	Manual	22059.23	35.40	7458.25	97.86	23284954.22	1605.35
	Automatic	22237.51	98.21	7678.41	232.56	23360609.38	6475.40
pDECO	Manual	22181.21	91.52	8176.00	163.45	25263415.89	4365.99
	Automatic	22865.41	254.92	8846.35	352.23	25407655.15	10972.48

Table 6: Average results (Cut values and run-times) of our proposed algorithms using the three datasets with two methods of selecting the hyper-parameters. First is using manually-tuned fixed parameters (denoted as “manual”), and the second is using the proposed evolution-based algorithm from Section 4.3.

C Baselines Detailed Implementation

For every baseline, we use the recommended default setting from their code base other than two methods: LwD and OptGNN.

For LwD [2], the code base only include the MIS problem. Therefore, we make the following modifications in the code. Each node’s label $s_i \in \{-1, 0, +1\}$ represents partition assignment, with 0 denoting undecided. At each stage the dual-head policy outputs (1) a defer decision $d_i \in \{0, 1\}$ indicating whether to assign node i now, and (2) an assignment $a_i \in \{+1, -1\}$ if $d_i = 1$. The observation per node is $[s_i, \mathbb{1}(s_i = 0), t/T_{\max}]$. Reward is the increment in cut value:

$$r_t = \text{Cut}(s^{(t)}) - \text{Cut}(s^{(t-1)}), \quad \text{where} \quad \text{Cut}(s) = \frac{1}{2} \sum_{(i,j) \in E} (1 - s_i s_j) \mathbb{1}(s_i \neq 0) \mathbb{1}(s_j \neq 0)$$

Policy optimization is performed with PPO using the joint log-probability of defer and assignment decisions; the surrogate loss, value loss, and entropy regularization follow standard formulations with clipping. For more information, see the LwD implementation in our code.

For OptGNN [36], since the official implementation does not release any pre-trained weights or model checkpoints, we train the model from scratch following the loss formulation in the original paper. We use Adam optimizer with a learning rate of 1×10^{-3} and train for 100 epochs.

For training data, we construct a large set of synthetic random graphs, since the original benchmarks (ER and Gset) are already used for evaluating other baselines and should be held out for fair comparison. Specifically:

- **ER graphs:** We generate 1000 random graphs with node sizes $n \in \{50, 100, 200, 500\}$ and edge probabilities $p \in \{0.1, 0.2, 0.3, 0.5\}$ using the NetworkX implementation.
- **d -regular graphs:** To improve robustness, we additionally generate 200 d -regular graphs with $d \in \{4, 8, 16\}$.

Validation is performed on a small subset of generated ER and regular graphs (5% of the training size). For testing, we strictly hold out all the ER and Gset instances that were used by the baselines (127 ER and 80 Gset graphs), together with our own 15 large-scale graphs.